Experimental vertical stability studies for ITER performance and design guidance

D.A. Humphreys,[a] T.A. Casper,[b] N. Eidietis,[a] M. Ferrara,[c] D.A. Gates,[d] I.H. Hutchinson,[c] G.L. Jackson,[a] E. Kolemen,[d] J.A. Leuer,[a] J. Lister,[e] L.L. LoDestro,[b] W.H. Meyer,[b] L.D. Pearlstein,[b] A. Portone,[f] F. Sartori,[g] M.L. Walker,[a] A.S. Welander,[a] S.M. Wolfe[c]

[a]General Atomics, P.O. Box 85608, San Diego, California 92186-5608, USA

[b]Lawrence Livermore National Laboratory, Livermore, California 94550, USA

[c]Massachusetts Institute of Technology, Cambridge, Massachusetts 02139, USA

[d]Princeton Plasma Physics Laboratory, Princeton, New Jersey, USA

[e]EPFL CRPP-Lausanne, Lausanne, Switzerland

[f]Fusion for Energy, Barcelona, Spain

[g]Euratom/UKAEA Fusion Association, Culham Science Centre, Abingdon, UK

e-mail contact of main author: dave.humphreys@gat.com

Abstract. Operating experimental devices have provided key inputs to the design process for ITER axisymmetric control. In particular, experiments have quantified controllability and robustness requirements in the presence of realistic noise and disturbance environments, which are difficult or impossible to characterize with modeling and simulation alone. This kind of information is particularly critical for ITER vertical control, which poses the highest demands on poloidal field system performance, since the consequences of loss of vertical control can be

severe. The present work describes results of multi-machine studies performed under a joint ITPA experiment (MDC-13) on fundamental vertical control performance and controllability limits. We present experimental results from Alcator C-Mod, DIII-D, NSTX, TCV, and JET, along with analysis of these data to provide vertical control performance guidance to ITER. Useful metrics to quantify this control performance include the stability margin and maximum controllable vertical displacement. Theoretical analysis of the maximum controllable vertical displacement suggests effective approaches to improving performance in terms of this metric, with implications for ITER design modifications. Typical levels of noise in the vertical position measurement and several common disturbances which can challenge the vertical control loop are assessed and analyzed.

PACS Nos.: 52.55.Fa, 52.55.Tn, 02.30.Yy, 89.30.Jj

1. Introduction

Axisymmetric stability control in ITER is expected to be challenging because the target operational scenarios can approach practical controllability limits, while the consequences of loss of control are potentially severe [1]. ITER scenarios require plasma elongation of $\kappa_x = 1.85$ along with a correspondingly high vertical instability growth rate, particularly at high values of internal inductance that can result during startup or in ohmic, L-mode, or high-q_{95} operations. The allowable number of worst-case unrecoverable vertical displacements is highly constrained in ITER due to blanket module and first wall stress/fatigue limits [2]. Sufficient control performance with adequate margins is thus critical to the success of ITER. We present results of experiments and analysis of operational experience in Alcator C-Mod, DIII-D, NSTX, TCV, and JET. These results include ITPA joint experiments coupled with ITER modeling and model validation, and suggest that improving the vertical control capability of the ITER baseline design may be important in order to provide robustness comparable to that of presently operating devices. Modeling and simulation includes use of the LLNL Caltrans code [3], the GA TokSys environment [4], and the MIT Alcasim environment [5]. The present study focuses on "machine-independent" performance metrics that describe the proximity to practical controllability limits rather than ideal stability boundaries.

Section 2 describes general axisymmetric control, ITER fundamental control characteristics, and the nature of the design problem. Useful metrics are discussed and related theoretical aspects are derived. Section 3 discusses the essential role of experiments in assessing and guiding the specification of performance-limiting phenomena such as noise and disturbances for ITER. Section 4 summarizes key experimental results from several devices and describes operational aspects of the experiments, along with analysis of the data for application to ITER. Section 5

presents conclusions, including implications of the collected experimental results and analysis for potential ITER design modifications.

2. ITER Vertical Stability Characteristics and Issues

The ITER baseline design uses the set of four outboard superconducting poloidal field (PF) coils PF2-PF5 to provide fast vertical stability control (figure 1). This control circuit (referred to as "VS1") has been calculated to provide sufficient control capability to stabilize the nominal ITER scenario as specified in the 2001 design [6]. However, advancement of the design process and a focus on the need for operational robustness arising from the recent ITER Design Review have suggested the need for more control capability. For example, experiments emulating ITER startup scenarios on DIII-D [7] and other major tokamaks [8] have demonstrated that the internal inductance can reach values above $\ell_i(3) \sim 1.2$ in the absence of sufficient early heating, higher than the baseline assumed maximum value of $\ell_i(3) \sim 1.0$, and potentially exceeding vertical control limit for the VS1 system [7].

Various design modifications have been suggested to augment the baseline ITER vertical control system [9]. For example, use of two inboard central solenoid (CS) coils, CS2U and CS2L, would significantly increase the control capacity. These coils (referred to as the "VS2" circuit) are located in positions which minimize the penetration time of radial field through the vacuum vessel, making them very effective for high frequency control of vertical position. Another possibility illustrated in figure 1 is the installation of a new set of fast, internal Cu axisymmetric coils. These coils may be integrated with a proposed new array of nonaxisymmetric coils intended to apply resonant magnetic perturbations in order to suppress ELMs in ITER. The new internal coils would be capable of applying stabilizing radial field at the plasma on the same timescale as the current response of the coils themselves, since the field would not have to diffuse through the vessel wall in this case. Although the wall still partially shields the amplitude of the field produced by in-vessel coils, there is little phase lag introduced.

Vertical stability experiments on operating devices have been executed to evaluate the augmented effectiveness resulting from coil sets comparable to the ITER VS1 and VS2 systems, as well as the necessity for additional control capability in ITER.

3. The Axisymmetric Stability Control Design Problem and Role of Experiments

A. System modeling for design

Design of control systems to stabilize the axisymmetric vertical instability requires sufficiently accurate modeling of the electromagnetic characteristics of the conducting structure and PF coils, as well as the destabilizing force associated with the application of a quadrupole field required to produce plasma elongation. The most common model representation of the axisymmetric dynamic system combines a plasma force balance equation with a first-order ordinary differential equation matrix circuit representation of Faraday's Law for all stabilizing conductors in the system [10]. The circuit equation becomes

$$M_{ss}\,\dot{I}_s + R_{ss}\,I_s + \frac{\partial \psi_{sp}}{\partial z}\dot{z} = V_s \quad , \tag{1}$$

where M_{ss} is the stabilizing conductor mutual inductance matrix, R_{ss} is the diagonal resistance matrix, $\partial\psi_{sp}/\partial z$ denotes the variation in flux at conductors due to plasma vertical displacement z, I_s and V_s are vectors of conductor currents and voltages, respectively, and $\dot{x}$ denotes the time derivative. The massless plasma "quasi-equilibrium" assumption requires vertical force balance so that

$$0 = \frac{\partial F_z}{\partial z}\dot{z} + \frac{\partial F_z}{\partial I_s}\dot{I}_s \;\Rightarrow\; \dot{z} = \frac{\left(\partial F_z/\partial I_s\right)}{\left(\partial F_z/\partial z\right)}\dot{I}_s \equiv \frac{\partial z}{\partial I_s}\dot{I}_s \quad , \tag{2}$$

where $\partial F_z/\partial z$ denotes the variation in vertical force on the plasma with vertical position, z, and $\partial F_z/\partial I_s$ denotes the variation in vertical force on the plasma with conductor currents.

Combining equations (1) and (2) yields

$$M_{ss}\,\dot{I}_s + R_{ss}\,I_s + \frac{\partial\psi_{sp}}{\partial z}\frac{\partial z}{\partial I_s}\,\dot{I}_s = \left(M_{\mathrm{ss}} + \frac{\partial\psi_{\mathrm{sp}}}{\partial z}\frac{\partial z}{\partial I_{\mathrm{s}}}\right)\dot{I}_{\mathrm{s}} + R_{\mathrm{ss}}\,I_{\mathrm{s}} = L_{*\mathrm{s}}\;\dot{I}_{\mathrm{s}} + R_{\mathrm{ss}}\,I_{\mathrm{s}} = V_{\mathrm{s}} \quad , \tag{3}$$

where $L_{*\mathrm{s}}$ is the effective inductance matrix including the effect of plasma motion. A central consequence of this equation is that the eigenvalues of the state matrix, $A \equiv -L_{*\mathrm{s}}R_{\mathrm{ss}}$, are all negative (reflecting stable eigenmodes) except for one. The single unstable eigenmode is the growth rate of the vertical instability, γ_{z}. Voltages applied to active coils can stabilize this instability by applying a radial field opposing plasma vertical displacements. Restoration of a given initial displacement requires sufficient voltage and current capability, as well as a sufficiently rapid response. These requirements are the fundamental system characteristics which must be defined in design of the vertical control system.

B. *Aspects of the Design Problem and the Role of Experiments*

The design problem can be divided into several aspects or "layers" of control performance. The operating regime (often called "scenario") layer is concerned with determining coil voltages and currents capable of producing the nominal scenario trajectory of equilibria. In addition to this, the system must be capable of handling normal operating variations about the nominal scenario trajectory (e.g. from variation in ℓ_{i} and β_{p} resulting from somewhat different impurity conditions). This layer of scenario variation robustness provides a further requirement on control performance beyond the nominal requirements. Beyond this requirement, the presence of noise and disturbances increases the control requirements still more. These "perturbation layer" requirements usually have specific dynamic characteristics which are significantly more demanding than both the nominal operating regime and the scenario variation requirements. For example, a disturbance such as an ELM or H-L back transition will apply a rapid timescale

perturbation to the plasma shape which must be rejected or restored within a certain time. Typically such disturbance requirements impose demand for higher voltage in order to provide the necessary speed of response. These events will often set the power supply response time as well. Beyond this perturbation layer lies the complex control layer of off-normal events. These events impose requirements on control response capability to enable recovery (when possible), to shift to an alternate operating regime (when full recovery is not possible), to execute an early normal shutdown or a "soft" (off-normal, but still relatively slow) shutdown, or in the worst case to execute a rapid shutdown (often including explicit action to mitigate disruption effects).

The focus of the physics and control performance requirement studies described here is the perturbation layer, which typically imposes the greatest demands on dynamic control characteristics. Rejection of disturbances in this performance layer is closely related to avoidance of off-normal events (including loss of control), and can therefore relate to both robustness to expected disturbances (e.g. ELMs, planned H-L back transitions) and to off-normal event disturbances (e.g. unplanned H-L back transitions or minor disruption from a large impurity influx).

In order to specify requirements for rejection or stable response to disturbances, the expected amplitudes and dynamic characteristics of these disturbances must be separately defined. While some fiducial definitions of these disturbances have been defined in various ITER design documents (e.g. [11]), it is not clear that these definitions represent a complete set, and it is not clear what level of robustness is required in general. One approach to specifying the robustness level needed for ITER is to analyze the capability of presently operating devices in regimes when loss of control is as rare as required in ITER. This requires describing the performance of present devices and ITER in terms of machine-independent control metrics.

C. Metrics

The levels of performance required by ITER are best specified in terms of appropriate metrics, which reflect key aspects of performance. One commonly employed and useful metric of control capability is the stability margin, denoted m_s, which is approximately the ratio of the unstable growth time to the wall penetration time, $m_s \sim \tau_g / \tau_w$. The stability margin can be thought of as describing the distance from the ideal stability limit (which occurs at $m_s = 0$). Although several forms of this metric have been defined over the years, a useful definition independent of any conductor resistances is given by

$$m_s \equiv \lambda_1 \left\{ M_{ss}^{-1} L_* \right\} \quad , \tag{4}$$

where $\lambda_1\{A\}$ represents the dominant eigenvalue of the matrix A, M_{ss} is the mutual inductance matrix for the set of stabilizing conductors including PF coils and a discretized representation of the passive conductors in the axisymmetric system. This definition of stability margin has been extensively applied to ITER [12] to assess and define performance requirements.

Because of differences in conducting structures, control coil configurations, and power supply dynamics, both required and attainable stability margins differ from device to device. For example, TCV operates above a minimum stability margin of $m_s(\min) \sim 0.10$, DIII-D above $m_s(\min) \sim 0.16$, and C-Mod above $m_s(\min) \sim 0.26$ (section 4). The absolute stability margin does not therefore reflect a machine-independent control requirement. More appropriate for inter-machine comparisons is the ratio $\tilde{m}_s \equiv m_s / m_s(\min)$, where $m_s(\min)$ is the practically attainable m_s for a given coil/structure configuration and power supply response. This ratio is therefore a measure of robustness in that it reflects the distance from the minimum practically controllable stability margin.

Another key metric of control performance is the maximum controllable displacement, which most directly quantifies the nonlinear constraints imposed by power supply limits. The gedanken experiment defining this metric is shown in figure 2, illustrating the plasma vertical position (Z) trajectory for different values of initial displacement. Control is disabled, and the plasma is allowed to move vertically by some distance, at which time commands to the power supplies used for vertical control are maximized to oppose the motion. Power supplies typically respond to this saturated command with a delay, then a slew rate-limited (or otherwise phase lagged) voltage rise, and eventually with a constant saturated voltage. For sufficiently large displacements, the power supply response and saturated voltage available will not be able to reverse the motion, and the instability will continue to grow. The maximum displacement for which this procedure can reverse the motion is defined as the maximum controllable displacement, denoted $\Delta Z_{\max}$. This metric is particularly useful in describing vertical control capability since the gedanken experiment that defines it mimics the destabilizing effect of a wide range of disturbances experienced in tokamaks, including ELMs and H-L transitions. The response to and tolerance of high amplitude noise in the vertical control loop are similarly quantified by the metric. Figure 2 represents a specific scan of displacement values for an ITER equilibrium occurring at the end of a simulated rampup scenario, using the VS1 control circuit only. This scan using the TokSys modeling environment results in $\Delta Z_{\max} \sim 0.04$ m for this equilibrium state. Various dimensionless forms of this quantity describe different machine-independent aspects of robustness, including $\Delta \tilde{Z}_a \equiv \Delta Z_{\max}/a$ (normalized by minor radius), or $\Delta \tilde{Z}_n \equiv \Delta Z_{\max}/\langle \Delta Z_{\text{noise}} \rangle_{\text{rms}}$ (normalized by the rms amplitude of the variation in measured vertical position). The former reflects general displacement robustness relative to machine geometry, while the latter specifically measures the margin relative to noise amplitude, which

often sets the limit of control. A value of $\Delta Z_{\max} \sim 0.04$ m corresponds to $\Delta \tilde{Z}_a \equiv \Delta Z_{\max}/a \sim 2\%$ in ITER.

A theoretical analysis of the maximum controllable displacement can help to quantify the relationship between this metric and key control aspects of various candidate designs for augmenting the ITER control system. Consider the circuit model description of axisymmetric control given by equations (1) through (3). Because such representations are typically of fairly high order (typically including ~30–100 coils and discretized conducting elements), they are usually solved numerically. However, an approximate solution can reveal the basic physics of the metric and quantify the performance consequences of various design options in the ITER control design.

The standard state space form of equation (3) is given by

$$L_{*\mathrm{s}}\ \dot{I}_\mathrm{s} + R_{\mathrm{ss}}\, I_\mathrm{s} = V_\mathrm{s} \ \Rightarrow\ \dot{I}_\mathrm{s} = AI_\mathrm{s} + BV_\mathrm{c} \quad , \tag{5}$$

where $V_\mathrm{s} = BV_\mathrm{c}$, and $B \equiv L_{*\mathrm{s}}^{-1}\vec{b}_\mathrm{c}$. V_c is a scalar voltage applied to the control coil (or to a control coil circuit assumed to be powered by a single power supply for the purposes of this analysis). $\vec{b}_\mathrm{c}$ is a vector (consisting of ±1s and 0s) mapping the control voltage to the correct control coil(s) circuit. Equation (5) defines an eigen value problem whose solution is given by

$$AV = V\Lambda \ \Rightarrow\ \Lambda = V^{-1}AV,\ A = V\Lambda V^{-1} \quad , \tag{6}$$

where V is the eigenvector matrix (whose columns are eigenvectors of A), and Λ is the diagonal eigenvalue matrix. The conductor current vector I_s can be expanded as a sum of weighted eigenvectors by defining $I_\mathrm{s} = Vw$, where w is a vector of weights (amplitudes of eigenvectors). Thus

$$\dot{w} = V^{-1}AVw + V^{-1}BV_c = \Lambda w + v_b V_c \quad . \tag{7}$$

Equation (7) implies the standard result that each mode is excited separately by the control circuit voltage V_c through an amplitude given by the elements of the vector $v_b \equiv V^{-1}B = V^{-1}L_{*s}^{-1}\vec{b}_c$.

The i[th] mode amplitude w_i evolves according to

$$\dot{w}_i = \lambda_i w_i + v_{bi}V_c \Rightarrow w_i(t) = e^{\lambda_i t}\int v_{bi}V_c e^{-\lambda_i t}dt + C_0 e^{\lambda_i t} \quad . \tag{8}$$

To derive an approximate solution that reveals the fundamental physics of the ΔZ_{max} metric, we focus on only three modes: the vertically unstable mode, the single mode dominated by the control coil response, and the passive structure mode with largest coupling to the control coil (which approximates the shielding of the control coil field by induced passive structure current). To determine the relevant initial condition for each mode amplitude, we consider the gedanken experiment defining the ΔZ_{max} metric illustrated in figure 2. This requires the application of a fully saturated voltage command after the plasma has moved a distance ΔZ_{max}, which results in a fully saturated voltage amplitude being applied (after some time T_{PS} for power supply response).

The control coil response to this saturated voltage is the key effect that must be modeled appropriately in order to derive a closed-form approximation to ΔZ_{max}. If the coil is resistive, the current response (ignoring coupling to other conductors) is of the form

$$I_c(t) = \frac{V_{sat}}{R_c}\left(1 - e^{-\gamma_c t}\right) \quad , \tag{9}$$

where V_{sat} is the saturation voltage, and $\gamma_c = R_c/L_c$. If the coil is superconducting, $R_c = 0$, and the evolution depends simply on the saturation voltage and inductance, so that $I_c(t) = \left(V_{sat}/L_c\right)t$.

In either case, there is a practical current limit setting the maximum value permissible (or attainable). In the resistive case, this may be the maximum coil current produced by the power

supply saturation voltage, $I_{max} = V_{sat}/R_c$, or some lower value. In the superconducting case, there will typically be an administrative limit on maximum current set by required margin relative to coil forces or quench limits. A useful model of power supply and coil response which captures the key dynamics of either situation, including a pure power supply delay, is shown in figure 3. A step command to the power supply (a) produces a pure delay (T_{PS}), after which the current response is modeled as a linear ramp with slope $\left(V_{sat}/L_c\right)$. For the purposes of vertical control we are concerned with the change in current from an initial equilibrium value (I_{equil}) to the maximum attainable. We denote this change in current by ΔI_{max} and it can be related to the ramp rate and the ramp time, T_c, via $\Delta I_{max} = \left(V_{sat}/L_c\right)T_c$. In order to approximate the resistive coil response of equation (7) we can choose $T_c = \left(L_c/R_c\right)$, and specify $\Delta I_{max} \simeq V_{sat}/R_c$ (assuming $V_{sat}/R_c >> I_{equil}$).

In the ΔZ_{max} gedanken experiment defining the metric (figure 2), and using this model for the power supply response, the unstable mode will have grown to amplitude w_{z0} corresponding to a vertical displacement ΔZ at the time the voltage command is saturated. Returning to equation (8), we define $t = 0$ as the time the coil current begins to ramp up (T_{PS} after the command is saturated). The initial condition at $t = 0$ is therefore that only the unstable mode w_z is non-zero, and that

$$w_z(t=0) = w_{z0}e^{\gamma_z T_{PS}} \quad . \tag{10}$$

The unstable mode evolution is given by

$$w_z = w_{z0}e^{\gamma_z (t+T_{PS})} - \frac{1}{\gamma_z} v_{bz} V_c \left(1 - e^{\gamma_z t}\right) \quad . \tag{11}$$

Under the representation used for both superconducting or resistive coils (figure 3), the control coil mode evolution is given approximately by

$$w_{\mathrm{c}} = v_{\mathrm{bc}} V_{\mathrm{c}} \approx \frac{V_{\mathrm{sat}}}{L_{\mathrm{c}}} t \quad , \tag{12}$$

where v_{bc} is the component of the vector v_{b} corresponding to the control coil mode. The dominant passive structure shielding mode evolves according to

$$w_{\mathrm{v}} = \frac{v_{\mathrm{bv}} V_{\mathrm{c}}}{\gamma_{\mathrm{v}}} \left(1 - e^{-\gamma_{\mathrm{v}} t}\right) \quad , \tag{13}$$

where v_{bv} is the component of the vector v_{b} corresponding to the dominant shielding mode, and $-\gamma_{\mathrm{v}}$ is the eigenvalue corresponding to that (stable) mode. The dominant shielding mode is that with maximum amplitude of the quantity $\left|v_{\mathrm{b}}/\gamma_{\mathrm{v}}\right|$ — excluding the unstable and control coil modes.

The vertical position trajectory is given by

$$z = \frac{\partial z}{\partial I_{\mathrm{s}}} I_{\mathrm{s}} = \frac{\partial z}{\partial I_{\mathrm{s}}} V w = \frac{\partial z}{\partial w} w$$

$$\simeq \frac{\partial z}{\partial w_{\mathrm{z}}} \left[w_{\mathrm{z0}} e^{\gamma_{\mathrm{z}} T_{\mathrm{PS}}} e^{\gamma_{\mathrm{z}} t} - \frac{1}{\gamma_{\mathrm{z}}} v_{\mathrm{bz}} V_{\mathrm{sat}} \left(1 - e^{\gamma_{\mathrm{z}} t}\right) \right] + \frac{\partial z}{\partial w_{\mathrm{c}}} \frac{V_{\mathrm{sat}}}{L_{\mathrm{c}}} + \frac{\partial z}{\partial w_{\mathrm{v}}} \left(1 - e^{-\gamma_{\mathrm{v}} t}\right) \quad . \tag{14}$$

When the available coil current is unlimited, the marginal displacement produces a linear trajectory corresponding to $\partial^2 z / \partial t^2 = 0$ [after the wall shielding mode, equation (13), has decayed], so that

$$\Delta Z_{\max} e^{\gamma_{\mathrm{z}} T_{PS}} + \frac{1}{\gamma_{\mathrm{z}}} \frac{\partial z}{\partial w_{\mathrm{z}}} v_{\mathrm{bz}} V_{\mathrm{sat}} = 0 \Rightarrow \Delta Z_{\max} = -\frac{\partial z}{\partial w_{\mathrm{z}}} v_{\mathrm{bz}} \frac{V_{\mathrm{sat}}}{\gamma_{\mathrm{z}}} e^{-\gamma_{\mathrm{z}} T_{\mathrm{PS}}} \quad . \tag{15}$$

Represented in terms of the plasma response to conductor currents, we obtain

$$\Delta Z_{\max} \approx -\frac{\partial z}{\partial I_{\mathrm{s}}} v_{\mathrm{z}} u_{\mathrm{z}} L_{*\mathrm{s}}^{-1} \vec{b}_{\mathrm{c}} \frac{V_{\mathrm{sat}}}{\gamma_{\mathrm{z}}} e^{-\gamma_{\mathrm{z}} T_{\mathrm{PS}}} \quad , \tag{16}$$

where v_z is the eigenvector corresponding to the unstable eigenmode, and u_z is the corresponding left eigenvector (defined by $u_z A = u_z \gamma_z$), which describes the degree to which the coil current evolution excites the unstable mode, a measure of controllability of the mode. Together, $\partial z/\partial I_s$ and u_z describe the effect of coil geometry on ΔZ_{max}. For example, in-vessel coils have higher control effectiveness than ex-vessel coils through these terms, and thus higher ΔZ_{max} values.

When the control coil current headroom is limited to ΔI_{max}, in the case of either superconducting or resistive coils, the value of ΔZ_{max}. is reduced to some value below the (effectively infinite ΔI_{max}) solution of equation (16). In this case we define the marginally controlled displacement ΔZ_{max} as that which produces a maximum in the $z(t)$ trajectory at the time the maximum current is reached. Setting the time derivative of equation (13) to zero to identify this point and requiring that $\Delta Z_{max} \to 0$ as $\Delta I_{max} \to 0$, we obtain an approximation for ΔZ_{max} under current limited conditions

$$\Delta Z_{max} \approx -\frac{\partial z}{\partial I_s} v_z u_z L_{*s}^{-1} \vec{b}_c \frac{V_{sat}}{\gamma_z} \left(1 - e^{-\frac{\Delta I_{max} L_c \gamma_z}{V_{sat}}} \right) e^{-\gamma_z T_{PS}} \quad . \tag{17}$$

Several useful observations proceed from these approximations to the maximum controllable displacement:

- ΔZ_{max} is directly proportional to the saturation voltage (and approximately inversely proportional to the active coil inductance).
- ΔZ_{max} is approximately inversely proportional to the growth rate, but also depends significantly on the $\gamma_z T_{PS}$ product roughly when $\gamma_z T_{PS} > 1$. This dependence quantifies

how fast the power supply must be so that its response does not limit control performance.

– Different control coil sets and power supply systems can be either voltage limited or current limited depending on their specific characteristics.
– When significantly limited by current headroom (roughly when $\Delta I_{\max} L_c \gamma_z / V_{sat} < 1$), $\Delta Z_{\max}$ is approximately proportional to the headroom $\Delta I_{\max}$.
– The scalar $(\partial z / \partial I_s) v_z u_z L_{*s}^{-1} \vec{b}_c$ quantifies the effectiveness of the control coil, including both geometrical and conducting structure shielding characteristics.

These observations imply that the saturation voltage is a strong design parameter which linearly influences the performance metric, while the strength of the dependence on growth rate itself depends on the power supply speed. For a sufficiently fast power supply ($T_{PS} \ll \gamma_z^{-1}$) details of the power supply response are unimportant. For example, the ITER baseline (VS1) vertical control system is driven by power supplies with overall response times of approximately 10 ms and maximum growth rate of approximately 20 rad/s (γ_z^{-1}= 50 ms), so that power supply response does not limit the VS1 performance [6,9]. Systems for which $\Delta I_{\max} L_c \gamma_z / V_{sat} >> 1$ are not limited by current capability, and can be said therefore to be voltage limited.

Evaluating the $\Delta Z_{\max}$ metric in ITER scenarios reveals important aspects of its performance. In contrast to the robust control (e.g. $\tilde{m}_s \sim 2$) found in ITER for the baseline design point, various other operating points likely to be accessed by ITER are calculated to have higher growth rates than the baseline design point, with correspondingly less controllability margin. For example, equilibria at the end of the reference ITER rampup scenario [7] are calculated by Corsica [3] (figure 4) and TokSys [4] (figure 2) to have $\Delta Z_{\max} \sim 4.0$ cm, corresponding to $\Delta \tilde{Z}_a \sim 2\%$. While simulations such as these can evaluate and compare performance for various

design choices and different scenarios, experimental data from operating devices is required in order to provide actual performance specifications (i.e. what level of ΔZ_{max} will be needed for operational robustness).

4. Experimental Results from Operating Devices

Tokamaks and spherical tori with vertically elongated plasmas are equipped to do studies of vertical controllability and robustness to provide the empirical results needed by ITER. Experimental data from several such devices have been analyzed to provide controllability guidance in terms of the metrics discussed in section 3.

A. Stability margin

The absolute stability margin values achieved in present devices vary significantly one from another, and are not necessarily appropriate targets for ITER. However, the relative stability margins at which these devices operate provide measures of robustness in terms of proximity to a controllability boundary (rather than to an ideal stability boundary). For example, typical robust operation in both DIII-D and Alcator C-Mod, including the ITER baseline point with $\ell_i(3) = 0.85$, corresponds to $\tilde{m}_s \sim 2$–3 [13] (figure 5). Calculations for ITER itself at the baseline point indicate $m_s \sim 0.70$ and $m_s(\min) \sim 0.37$, corresponding to comparable $\tilde{m}_s \sim 2$ and thus a comparable robustness level. Note that growth rate increases with both elongation of the last closed flux surface κ_x (also denoted κ_a in figure 5) and internal inductance $\ell_i(3)$.

B. Maximum controllable vertical displacement $\Delta Z_{\max}$

Modeling of DIII-D and Alcator C-Mod control performance shows that operation with calculated $\Delta\tilde{Z}_a \sim 2\%$ in both devices corresponds to assured loss of control, while $\Delta\tilde{Z}_a \sim 4\%$ corresponds to marginal controllability. For example, table I summarizes vertical stability characteristics of a sequence of equilibria in Alcator C-Mod. The last row, with calculated $\Delta\tilde{Z}_a \sim 4\%$, corresponds to marginal controllability with high likelihood of loss of vertical control. Figure 6 shows a typical DIII-D controllability threshold experiment, in which the

elongation was increased steadily until the plasma was lost vertically. Below a calculated value of $\Delta\tilde{Z}_a \sim 4\%$ [$\Delta Z_{\max} \sim 2.3$ cm; solid horizontal red line (Fig. 6(b)] the positional regulation becomes progressively degraded, as the voltage command saturates for increasingly long periods, but stability is not lost. At $\Delta\tilde{Z}_a \sim 2\%$ {$\Delta Z_{\max} \sim 1.2$ cm; dashed red line [Fig. 6(b)] and solid vertical red line [Fig. 6(b,c)]} the vertical control is completely lost and a VDE develops. The fact that both C-Mod and DIII-D frequently operate in the range of (calculated) $\Delta\tilde{Z}_a \sim$ 5–10% with no loss of vertical control in the absence of large disturbances or control-compromising off-normal events, but experience very likely loss of vertical control below $\Delta\tilde{Z}_a \sim$ 2% suggests that if ITER experiences a similar disturbance and noise environment to these two devices, achievement of comparable robustness of vertical control in ITER may require similar maximum controllable displacement capability above ~5% of the minor radius. However, in order to apply this experience to the ITER design with confidence, benchmarking of these calculated values against experimentally observed values is highly desirable.

Experiments performed on several devices in 2007–08 under ITPA joint experiment MDC-13 have obtained direct measurements of the maximum controllable displacement by triggering uncontrolled vertical drifts in order to compare to calculations. The experiment calls for turning off vertical control for varying periods, and allowing different distances of drift before applying a command to fully saturate the control circuit voltage to oppose the direction of motion. Most operating devices have high enough gain in this control circuit that simply re-establishing control at the designated time produces the desired voltage saturation.

Experiments in Alcator C-Mod (figure 7) varying the elongation (and thus growth rate) in lower single null plasmas find the practically controllable $\Delta Z_{\max}$ to be close to but somewhat smaller than that derived from calibrated Alcasim simulations. For the highest growth rate case

studied, the experimental minor radius-normalized maximum controllable displacement is found to lie in the range of $\Delta\tilde{Z}_a \sim 0-5\%$. The upper bound of calculated values for the collection of equilibria of this elongation ($\kappa \sim 1.80$) is found to be $\Delta\tilde{Z}_a \sim 10\%$. Possible sources of discrepancy include power supply noise in the experiments, which is unaccounted for in the fundamental controllability calculation. Such sources of noise can perturb the vertical position during the growth of the instability and contribute to uncertainty in determining $\Delta Z_{\max}$. It is interesting to note that the Alcator C-Mod vertical control system is an example of a current-limited system, as described in section 3: the maximum controllable displacement is set by the current limit rather than the voltage saturation limit, as is also true of the in-vessel vertical control coils presently under consideration by ITER.

Experiments in NSTX have shown that a typical, highly robust double null plasma target has measured $\Delta Z_{\max} \sim 0.24 \pm 0.08$ m, corresponding to $\Delta\tilde{Z}_a \sim 37\% \pm 12\%$. Data from a scan of drift distances are summarized in figure 8, and show that upward and downward-directed drifts have approximately the same maximum controllable displacement. The filled region indicates the span between the maximum controlled and minimum uncontrolled displacement in each direction, although there is some ambiguity in the latter measurement owing to interaction with the wall, resulting in significant equilibrium change. Interaction with the limiter occurs at $\Delta Z \sim 0.24$ m, as incidentally corresponding to the mean value of the inferred range for $\Delta Z_{\max}$. However, the first case in which the plasma is completely lost vertically occurs at $\Delta Z \sim 0.32$ m ($\Delta\tilde{Z}_a \sim 50\%$). The maximum displacement calculated for this equilibrium and control configuration using a TokSys model developed in a collaboration between DIII-D and NSTX is found to be ~0.37 m, or $\Delta\tilde{Z}_a \sim 57\%$ (30% above the experimental mean, 7% above the first data point confirmed to be uncontrollable). The magnitude of even a 7% discrepancy, corresponding to 0.045 m, is far

greater than any observed sources of noise, and so is unlikely to be explained by such effects. More likely contributors to the discrepancy include inaccuracies in modeling the complex nonaxisymmetric passive structures of NSTX and nonlinear effects from the plasma striking the first wall. Understanding the effects of such nonaxisymmetries and nonlinearities on ΔZ_{max} may also be important for ITER.

Experiments in DIII-D have compared vertical control capability using an array of four outboard coils only (much like the ITER VS1 circuit) with the standard DIII-D vertical control array, which uses two inboard off-midplane coils (much like the ITER VS2 circuit) in addition to the outboard coils. Data from a scan of drift distances over a range of growth rates in lower single null plasmas are summarized in figure 9. Displacements that were controlled using the DIII-D VS1+VS2-like coil array are denoted by circles, and uncontrollable displacements using this array are denoted by x's. The calculated ΔZ_{max} values for this configuration and the range of growth rates shown are represented by the solid line. Displacements that were controlled using the DIII-D VS1-like coil array are denoted by diamonds, and uncontrollable displacements using this array are denoted by triangles. The corresponding calculated ΔZ_{max} values are represented by the dashed line. The VS1+VS2 array approximately doubles the ΔZ_{max} performance of the VS1 array alone. Although there is reasonable overall agreement with the data, the local discrepancies for both coil arrays reflect significant variability in measured vs calculated ΔZ_{max}.

The present ITER design is based on directly calculated or simulation-derived assessment of vertical control capability. The operational results studied here show broad agreement between calculated and experimentally derived values of ΔZ_{max}, but with varying degrees of accuracy. This difficulty in matching experimental values with calculations highlights the importance of

providing margin in the ITER control design based on calculated ΔZ_{max} performance assessments guided by experimental data. It should be noted that the variability in operational or experimental values of ΔZ_{max} from machine to machine simply reflects the different sizes, aspect ratios, specific equilibria, and operational choices of each device. Only the comparison with model-based calculations and the empirical limits to control are specifically relevant for ITER design guidance.

C. *Noise and its effect on* ΔZ_{max}

Although we have chosen to relate ΔZ_{max} to the minor radius in order to provide an approximate machine-independent metric, the actual controllability limit must be set by a combination of the typical noise and disturbance environments of each device. We focus here on the total standard deviation of the vertical position measurement, including all sources of noise and disturbance (power supplies, instrumentation, aliasing, signal cross-talk, plasma instabilities, etc.) and compare it to the calculated ΔZ_{max} in loss of control cases. Table II summarizes typical noise standard deviations in several devices operating routinely at vertical elongations comparable to or greater than that expected for ITER. These vertical position measurement standard deviations are remarkably consistent, typically falling in the range of 0.5%–1% of the plasma minor radius in each device. A significant exception is TCV, which underwent a careful and systematic process to minimize the system noise. It should be noted that all of these devices report some degree of variation in standard deviation of this signal, depending on physical operating regime, presence of MHD instabilities, plasma shape, etc. The values given are reported “typical” values for a range of L- and H-mode plasmas, assessed in periods without ELMs or other large-scale disturbances.

If ITER were to experience similar levels of signal variance as a fraction of minor radius as found in presently operating devices, it is likely that ITER would find a similar (assumedly noise-driven) value of $\Delta Z_{\max}/a \sim 4\%$ for marginal controllability, with $\Delta Z_{\max}/a \sim 2\%$ corresponding to high probability of VDE (vertical displacement event: an unrecoverable loss of vertical control). Beyond a statistical survey such as this, it is difficult to assess the level of variance expected in the ITER vertical position measurement. However, data from operating devices can provide some information relating empirical controllability limits to $\Delta Z_{\max}$, and the position measurement standard deviation. Table I shows (last column, bottom row) that the marginal control case corresponds to a ratio of $\Delta Z_{\max}/\langle Z \rangle$ rms ~ 8 in Alcator C-Mod. Figure 10 summarizes a DIII-D experiment in which the plasma elongation was steadily increased in an upper single null plasma until an uncontrollable VDE occurred. The calculated growth rate is shown increasing in figure 10(b), as $\Delta Z_{\max}$ decreases figure 10(c). The previously identified point of marginal control robustness is identified by a solid (red) line ($\Delta Z_{\max} \sim 2.4$ cm, $\Delta Z_{\max}/a \sim 4\%$), and the point at which vertical control is lost is identified by a dashed (red) line. The ratio of $\Delta Z_{\max}/\langle Z \rangle$ rms ~ 5 corresponding to the marginal controllability point and $\Delta Z_{\max}/\langle Z \rangle$ rms ~ 2 corresponding to loss of control are denoted by (red) solid and dashed lines respectively in figure 10(e).

5. Summary and Conclusions

Experimental results from presently operating devices are essential to provide guidance on ITER control robustness requirements. Statistical analysis of experimental databases and recent experiments to mimic ITER startup suggest that ITER is likely to achieve internal inductance values in excess of $\ell_i(3) = 1.2$, which would challenge the baseline vertical control system. Reported operational experience in DIII-D and Alcator C-Mod, including recent ITPA joint experiments, implies that they must achieve maximum controllable displacement levels above ~5% of the minor radius to avoid loss of vertical control. If the ITER noise and disturbance environment is comparable to these operating devices (as a fraction of minor radius), these results suggest that achievement of comparable robustness of vertical control in ITER may require similar maximum controllable displacement capability above ~5% of the minor radius. In fact, present devices most frequently operate with maximum controllable displacement in the range of 10% or above, with no measurable risk of vertical control loss in the absence of a significant off-normal event such as a power supply failure. Comparisons of calculated values with experimentally measured values of maximum controllable displacement show reasonable agreement, but with significant variability, reinforcing the need for margin in ITER design capability. Experimental studies show that in DIII-D an ITER-like "VS1+VS2" coil set provides approximately twice the ΔZ_{max} performance of an ITER-like VS1-only coil set. The typical standard deviations $\langle Z \rangle$ rms of vertical position measurement signals in many devices lie in the range of 0.5%–1.0% of the minor radius. Marginal controllability corresponds to $\Delta Z_{max} / \langle Z \rangle \mathrm{rms} \sim 5 - 8$, while ensured loss of control is found to occur when $\Delta Z_{max} / \langle Z \rangle \mathrm{rms} \sim 2$. Further experimental work and analysis is needed in order to evaluate the effects of various disturbances and quantify ITER performance metrics in terms of these effects. Analysis of

control capabilities in other highly shaped tokamaks continues to be needed in order to improve confidence in the robustness metrics evaluated here as useful specifications of required control performance.

Acknowledgment

This work was supported by the US Department of Energy under DE-FC02-04ER54698, DE-AC52-07NA27344, and DE-FG02-04ER54235. This report was prepared as an account of work by or for the ITER Organization. The Members of the Organization are the People's Republic of China, the European Atomic Energy Community, the Republic of India, Japan, the Republic of Korea, the Russian Federation, and the United States of America. The views and opinions expressed herein do not necessarily reflect those of the Members or any agency thereof.

References

[1] Chapter 1: overview and summary, from *Progress in the ITER Physics Basis*, M. Shimada *et al* eds. 2007 *Nucl. Fusion* **47** S1

[2] Sugihara M *et al* 2007 *Nucl. Fusion* **47** 337

[3] Crotinger J A *et al* 1997 CORSICA: A comprehensive simulation of toroidal magnetic-fusion devices, Lawrence Livermore National Laboratory, Technical Report UCRL-ID-126284, available from NTIS #PB2005-102154

[4] Humphreys D A *et al* 2007 *Nucl. Fusion* **47** 943

[5] Ferrara M 2006 Alcasim simulation code for Alcator C-Mod, *Proc. 45th IEEE Conf. on Decision and Control*, *San Diego, California*. p. 2238.

[6] ITER Final Design Report 1998 International Atomic Energy Agency, Vienna, Austria, IAEA Document IAEA/ITER-EDA/DS/16

[7] Jackson G L, Casper T A, Luce T C, Humphreys D A, Ferron J R, Petrie T W and West W P 2008 Simulating the ITER plasma startup scenario in the DIII-D tokamak, *submitted for publication in Nucl. Fusion*

[8] Sips A C C *et al* 2008 *Nucl. Fusion* **49** 085015

[9] Portone A *et al* 2008 ITER plasma vertical stabilization, in Fusion Energy 2008 (*Proc. 22nd IAEA Fusion Energy Conf., Geneva, 2008) (Vienna: IAEA)* CD-ROM file IT/R2-4Ra and http:/www-naweb.iaea.org/napc/physics/FEC/FEC2008/html/index.htm

[10] Portone A *et al* 1997 *Fusion Technol.* **32** 374

[11] Gribov Y *et al* 2007 Chapter 8: plasma operation and control, from *Progress in the ITER Physics Basis*, M. Shimada *et al* eds *Nucl. Fusion* **47** S385

[12] Portone A 2005 *Nucl. Fusion* **45** 926

[13] Ferrara M, Hutchinson I H and Wolfe S M 2008 *Nucl. Fusion* **48**, 065002

Table I: Summary of vertical stability characteristics for sequence of increasingly unstable Alcator C-Mod equilibria.

Case	γ_z (rad/s)	m_s	ΔZ_{max} (cm)	$\Delta Z_{max}/a$ (%)	$\Delta Z_{max}/\langle \Delta Z_{noise} \rangle$
1	210	0.41	2.8	13.0	28
2	260	0.35	2.1	9.7	21
3	310	0.32	1.5	6.9	15
4	410	0.28	0.8	3.7	8

Table II. Summary of typical standard deviation in vertical position measurement signal noise for many devices.

Device	Typical $\langle Z \rangle$ rms (cm)	Minor Radius, a (cm)	$\langle Z \rangle / a$ (%)
Alcator C-Mod	0.10	21	0.5
DIII-D	0.3–0.5	60	0.5–0.8
JET	1.4	100	1.4
NSTX	0.7	63	1.1
TCV	0.05	25	0.2

Figure Captions

Fig. 1. (Color On-Line ONLY) ITER poloidal cross-section geometry and vertical control system options.

Fig. 2. (Color On-Line ONLY) Illustration of gedanken experiment defining maximum controllable displacement ΔZ_{max}. Simulation corresponds to ITER end-of-rampup state with $\Delta Z_{max} \sim 4$ cm, $\Delta Z_{max}/a \sim 2\%$.

Fig. 3. (Color On-Line ONLY) Power supply and coil model step response current history.

Fig. 4. (Color On-Line ONLY) Corsica simulations of ITER ΔZ_{max} scenario for end-of-rampup scenario, $\ell_i(3) = 1.0$, show ITER maximum controllable displacement of 3.5 cm, corresponding to ~2% of the ITER minor radius.

Fig. 5. (Color On-Line ONLY) Alcator C-Mod/DIII-D stability margins for ITER similar equilibria.

Fig. 6. (Color On-Line ONLY) DIII-D controllability threshold experiment. (a) shows growth rate increasing as the elongation is increased. (b) shows calculated ΔZ_{max} decreasing at the same time. The solid red horizontal line (b) and solid black vertical lines (b,c) indicate the point at which the vertical control command is fully saturated for increasingly long periods and control becomes marginal. The dashed red horizontal line (b) and solid red vertical line (b,c) indicate the point at which vertical control is actually lost and a vertical displacement event (VDE) begins, corresponding to $\Delta Z_{max}/a \sim 2\%$.

Fig. 7. (Color On-Line ONLY) Summary of Alcator C-Mod experiment measuring $\Delta Z_{\max}$ as a function of elongation at the separatrix. The blue solid line indicates the experimentally estimated maximum controllable displacement, while the red dashed line indicates the values derived from simulations calibrated to the experimental growth rates.

Fig. 8. (Color On-Line ONLY) Summary of NSTX experiment measuring $\Delta Z_{\max}$. Light grey regions indicate uncontrollable displacements inferred from the minimum experimentally uncontrolled value. White region indicates controllable displacements inferred from the maximum unambiguously controlled value. Orange (dark gray) indicates the uncertain range containing the experimentally determined $\Delta Z_{\max}$. Horizontal red line indicates the calculated value of $\Delta Z_{\max}$.

Fig. 9. (COLOR) Summary of DIII-D experiment measuring $\Delta Z_{\max}$. The figure shows vertical displacements as a function of fitted growth rate. Solid blue line denotes the calculated $\Delta Z_{\max}$ as a function of growth rate for the DIII-D VS1+VS2-like coil set. The dashed blue line indicates the calculated $\Delta Z_{\max}$ for the DIII-D VS1-like coil set alone.

Fig. 10. (Color On-Line ONLY) Summary of DIII-D experiment assessing the ratio of $\Delta Z_{\max}$ to the rms noise amplitude, $\Delta Z_{\max}/\langle Z\rangle$rms at the limit of controllability. The solid red (gray) line corresponds to the previously identified point of marginal stability ($\Delta Z_{\max}/a \sim 4\%$, $\Delta Z_{\max}/\langle Z\rangle_{\rm rms} \sim 5$), while the dashed red (gray) line indicates the point at which vertical control is lost ($\Delta Z_{\max}/a \sim 2\%$, $\Delta Z_{\max}/\langle Z\rangle_{\rm rms} \sim 2$).

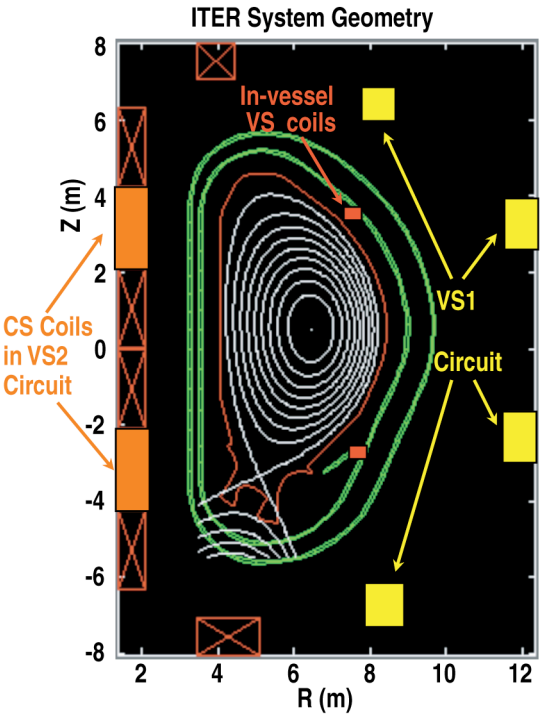

Fig. 1, D.A. Humphreys

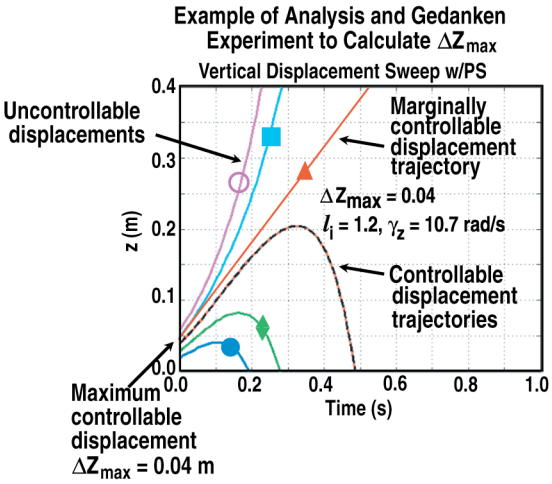

Fig. 2, D.A. Humphreys

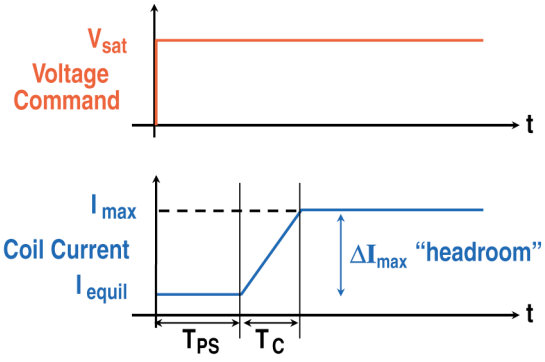

Fig. 3, D.A. Humphreys

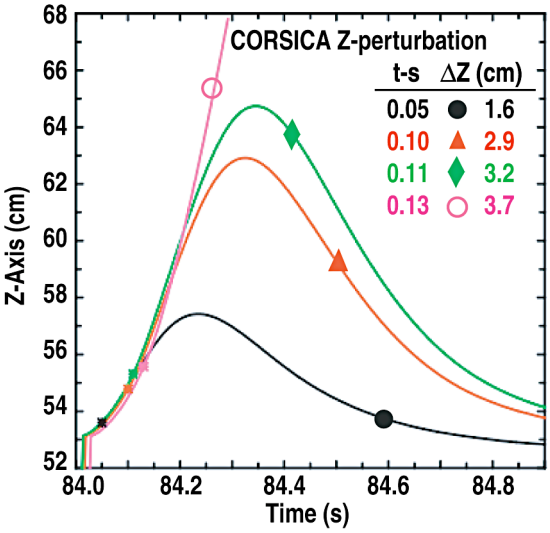

Fig. 4, D.A. Humphreys

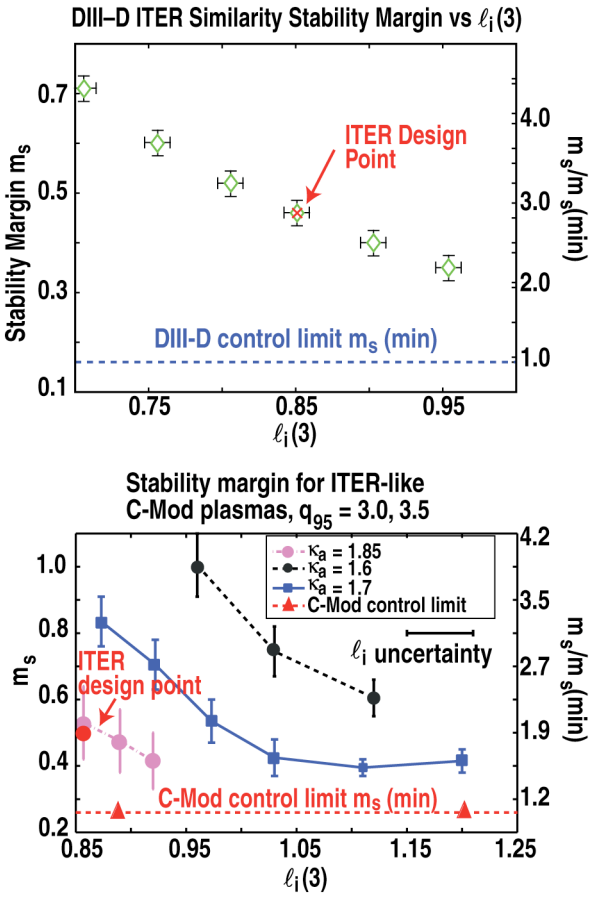

Fig. 5, D.A. Humphreys

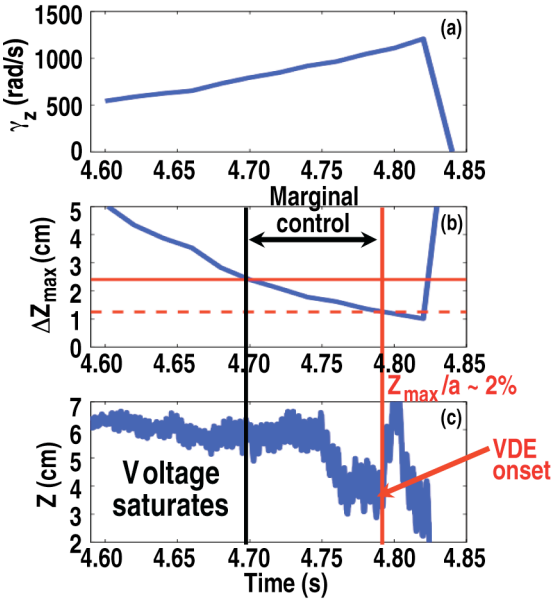

Fig. 6, D.A. Humphreys

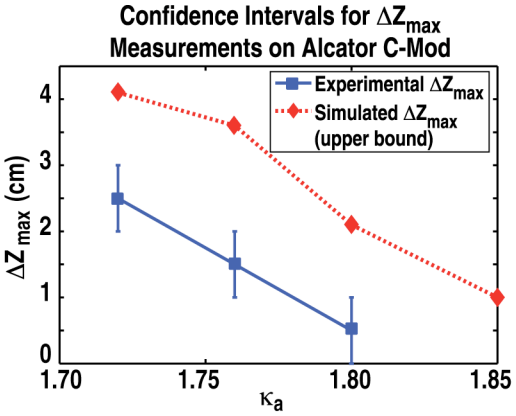

Fig. 7, D.A. Humphreys

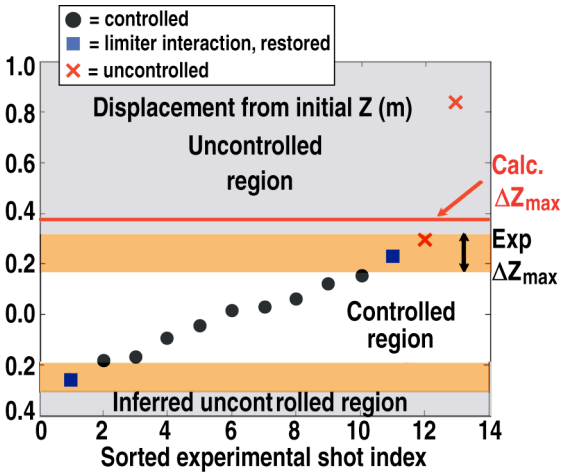

Fig. 8, D.A. Humphreys

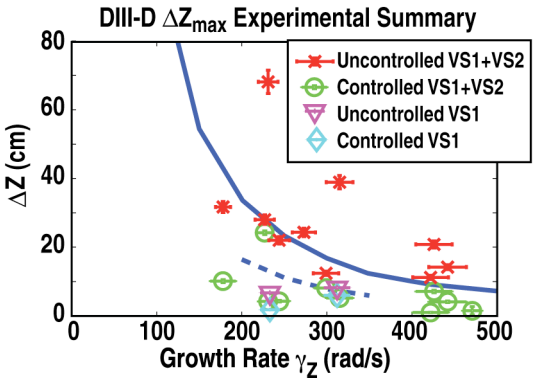

Fig. 9, D.A. Humphreys — COLOR

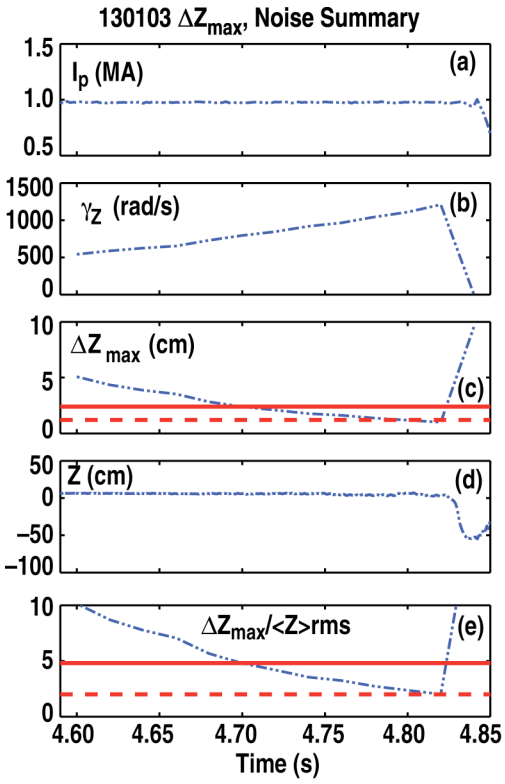

Fig. 10, D.A. Humphreys